


Comparison of Prospectively Generated Glioma Treatment Plans Clinically Delivered on Magnetic Resonance Imaging (MRI)-Linear Accelerator (MR-Linac) Versus Conventional Linac: Predicted and Measured Skin Dose

Technology in Cancer Research & Treatment
Volume 21: 1-10
© The Author(s) 2022
Article reuse guidelines:
sagepub.com/journals-permissions
DOI: 10.1177/15330338221124695
journals.sagepub.com/home/tct


Michael H. Wang, MD¹, Anthony Kim, PhD^{1,2}, Mark Ruschin, PhD^{1,2}, Hendrick Tan, MD¹, Hany Soliman, MD¹, Sten Myrehaug, MD¹, Jay Detsky, MD, PhD¹, Zain Husain, MD¹, Eshetu G. Atenafu, MSc³ , Brian Keller, PhD^{1,2}, Arjun Sahgal, MD¹, and Chia-Lin Tseng, MD¹ 

Abstract

Introduction: Magnetic resonance imaging-linear accelerator radiotherapy is an innovative technology that requires special consideration for secondary electron interactions within the magnetic field, which can alter dose deposition at air–tissue interfaces. As part of ongoing quality assurance and quality improvement of new radiotherapy technologies, the purpose of this study was to evaluate skin dose modelled from the treatment planning systems of a magnetic resonance imaging-linear accelerator and a conventional linear accelerator, and then correlate with in vivo measurements of delivered skin dose from each linear accelerator. **Methods:** In this prospective cohort study, 37 consecutive glioma patients had treatment planning completed and approved prior to radiotherapy initiation using commercial treatment planning systems: a Monte Carlo-based algorithm for magnetic resonance imaging-linear accelerator or a convolution-based algorithm for conventional linear accelerator. In vivo skin dose was measured using an optically stimulated luminescent dosimeter. **Results:** Monte Carlo-based magnetic resonance imaging-linear accelerator plans and convolution-based conventional linear accelerator plans had similar dosimetric parameters for target volumes and organs-at-risk. However, magnetic resonance imaging-linear accelerator plans had 1.52 Gy higher mean dose to air cavities ($P < .0001$) and 1.10 Gy higher mean dose to skin ($P < .0001$). In vivo skin dose was 14.5% greater for magnetic resonance imaging-linear accelerator treatments ($P = .0027$), and was more accurately predicted by Monte Carlo-based calculation ($\rho = 0.95$, $P < .0001$) versus convolution-based ($\rho = 0.80$, $P = .0096$). **Conclusion:** This is the first prospective dosimetric comparison of glioma patients clinically treated on both magnetic resonance imaging-linear accelerator and conventional linear accelerator. Our findings suggest that skin doses were significantly greater with magnetic resonance imaging-linear accelerator plans but correlated better with in vivo measurements of actual skin dose from delivered treatments. Future magnetic resonance imaging-linear accelerator planning processes are being designed to account for skin dosimetry and treatment delivery.

Keywords

MRI-guided radiotherapy, MR-Linac, skin dose, interface effects, electron return effect, Monte Carlo

¹ Department of Radiation Oncology, Sunnybrook Odette Cancer Centre, University of Toronto, Toronto, Ontario, Canada

² Department of Medical Physics, Sunnybrook Odette Cancer Centre, University of Toronto, Toronto, Ontario, Canada

³ Department of Biostatistics, University Health Network, University of Toronto, Toronto, Ontario, Canada

Corresponding Author:

Chia-Lin (Eric) Tseng, MD, Department of Radiation Oncology, University of Toronto, Odette Cancer Centre, Sunnybrook Health Sciences Centre, 2075 Bayview Avenue, Toronto, Ontario, Canada M4N 3M5.

Email: chia-lin.tseng@sunnybrook.ca



Abbreviations

CBCT, cone beam CT; CI, conformity index; CTV, clinical target volume; DVH, dose-volume histogram; ERE, electron return effect; GI, gradient index; GTV, gross tumor volume; HI, homogeneity index; IMRT, intensity-modulated radiation therapy; MRI, magnetic resonance imaging; MR-Linac, MRI-linear accelerator; OARs, organs-at-risk; OSLD, optically stimulated luminescent dosimeter; PTV, planning target volume; TPS, treatment planning system.

Received: May 9, 2022; Revised: August 3, 2022; Accepted: August 19, 2022.

Introduction

Modern radiotherapy with selective use of magnetic resonance imaging (MRI) during the treatment course has shown promise for evaluating glioma tumor dynamics,¹ predicting glioma treatment response² and identifying regions for dose escalation based on functional imaging. Typically, no more than 2 to 3 MR images are obtained during a 6-week radiation treatment course due to practicalities and costs of repeat MRIs. The advent of integrated MRI-linear accelerator (MR-Linac) systems enables daily acquisition of high field strength (1.5 Tesla) diagnostic quality MRI to facilitate adaptive radiotherapy, to individualize radiation treatment plans and to incorporate functional imaging. At our institution, we have been developing the application of the Unity MR-Linac (Elekta AB) to brain tumors, and have treated over 150 glioma patients using either 3 or 6 weeks of daily fractionated standard radiotherapy with concurrent temozolomide.

The challenge of delivering radiation within a high MRI field strength environment is the influence of the Lorentz force on dose deposition. The electron return effect (ERE) refers to secondary electrons exiting tissue into air being curved back to deposit dose at the tissue surface due to the Lorentz effect, which results from the presence of the strong magnetic field placed perpendicularly to the beam direction.^{3–11} Until now, ERE has been investigated in phantom studies,¹² and in simulated dosimetric studies^{13–17} with research versions of MR-Linac planning software prior to the release of the current clinical treatment planning version. Assessment of skin dose is important in radiotherapy for glioma patients because of the potential for dose-related clinical toxicities, and as a component of ongoing quality assurance and quality improvement of new radiotherapy technologies.

In this prospective dosimetric study, our objective was to investigate glioma patients treated on the prospective MOMENTUM trial¹⁸ who received at least one fraction of radiotherapy on both the MR-Linac and a conventional Linac (Elekta AB): (1) the dosimetric impact of the MR-Linac's magnetic field on the target, organs-at-risk (OARs), skin and tissues surrounding air cavities, and; (2) to compare skin dose modelled from the treatment planning software with in vivo skin dose measurements.

Patients and Methods

This prospective cohort study has been approved by the research ethics board of Sunnybrook Health Sciences Centre

(Toronto, Canada) until March 3, 2023 (Study Number: 3039). The design and reporting of this study conforms to established STROBE guidelines,¹⁹ and all patient details were de-identified for analysis and presentation in this manuscript. Consecutive glioma patients starting radiotherapy between July 2019 and February 2021 provided informed written consent prior to enrollment on the prospective MOMENTUM trial. All patients completed maximal safe surgical resection followed by either 3 or 6 weeks of adjuvant radiotherapy according to standard practices.^{20, 21} Patients were treated on the Unity MR-Linac (Elekta AB) and our standard practice was to create a clinical backup plan on a conventional cone beam CT (CBCT)-guided Linac equipped with the Agility head (Elekta AB) during treatment planning. On days when the MR-Linac was scheduled for maintenance or had a service issue such that treatment would otherwise be delayed, patients were irradiated on the conventional Linac for that particular radiotherapy fraction. All MR-Linac treatment plans and conventional Linac clinical backup plans were generated as per standard of care and deemed clinically acceptable prior to initiation.

All patients were simulated with a treatment planning CT (Brilliance, Philips Healthcare) with a slice thickness of 1.0 mm, and immobilized with a thermoplastic head immobilization mask (CIVCO Medical Solutions). MRI simulation at 1.5 Tesla (Ingenia, Philips Healthcare) was also performed in the treatment position with the immobilization mask applied. Standard volumetric axial T1 gadolinium-enhanced and T2 FLAIR sequences with a slice thickness of 1.0 mm were acquired. CT images and MRI sequences were registered and fused based on rigid mutual information registration within a region of interest box defined around the tumor.²²

Treatment planning for the MR-Linac was completed on the Monaco treatment planning system (TPS) (Monaco v5.40, Elekta AB). Delineation of OARs, gross tumor volume (GTV), and clinical target volume (CTV) were defined based on glioma consensus contouring guidelines.²³ Planning target volume (PTV) was generated as a 4-mm isotropic expansion of the CTV. The Monte Carlo algorithm²⁴ accounts for magnetic field effects for the MR-Linac. A TPS based on a convolution-superposition dose calculation algorithm (Pinnacle v9.8, Philips Healthcare) was used for planning on the conventional Linac (Figure 1). All efforts to accurately model skin surface dose using Monaco and Pinnacle were independently benchmarked, and beam models were all commissioned as per TG-53 and TRS-430 guidelines, which recommended dose and spatial tolerances for percentage

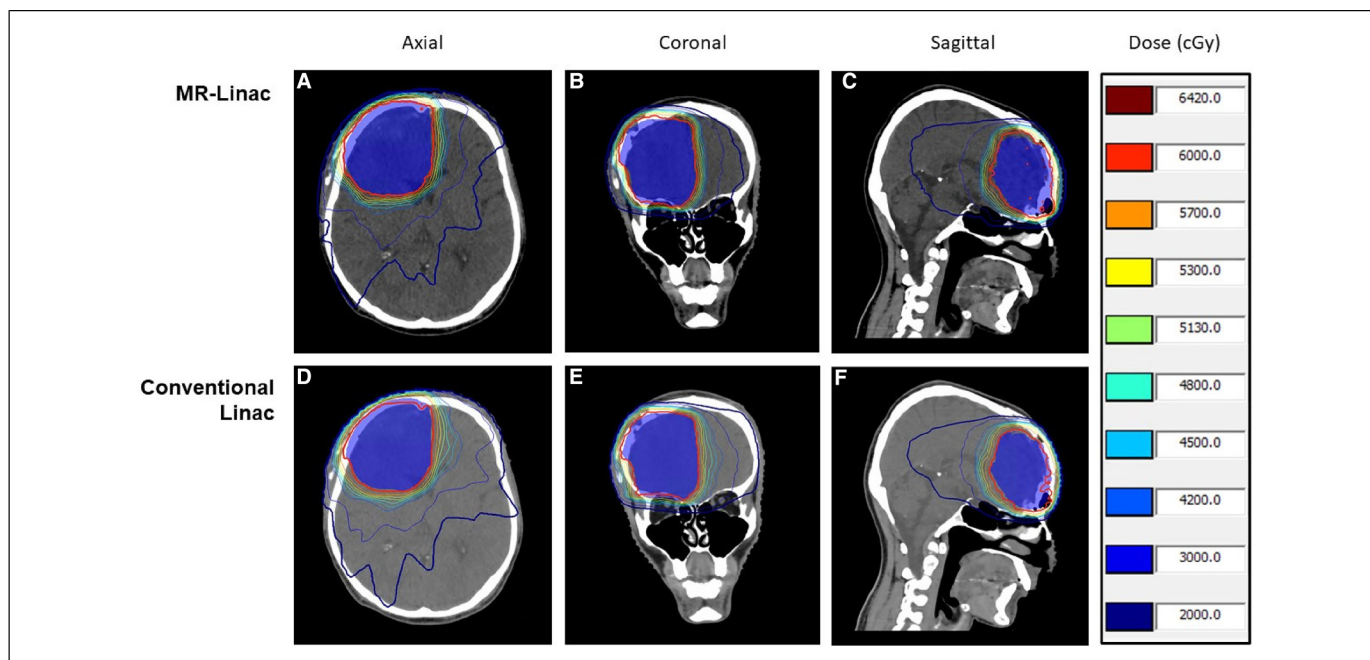


Figure 1. Clinically delivered treatment plans for a representative study patient diagnosed with glioblastoma, and prescribed 60 Gy in 30 fractions. Top row depicts MR-Linac axial (A), coronal (B), and sagittal (C) dose distributions from Monaco. Bottom row depicts conventional Linac axial (D), coronal (E), and sagittal (F) dose distributions generated from Pinnacle. PTV is depicted in blue colorwash. Multi-color isodose lines are quantified in cGy.

depth dose and penumbra for a range of field sizes within the beam, outside of the beam, in the penumbra, and at the surface. In particular, Monaco's Monte Carlo dose calculation algorithm has superior agreement when compared to Pinnacle's convolution-superposition dose calculation algorithm in quantifying measured dose compared to TPS dose in the buildup region.⁹

MR-Linac plans used ≥ 9 coplanar non-opposing step-and-shoot Intensity-Modulated Radiation Therapy (IMRT) 7 MV photon beams, with a maximum dose rate of 425 MU/min, and beam collimation using 80 MLC leaf pairs with a leaf width of 7.175 mm at isocenter. Plans were optimized to achieve at least 90% of the prescription dose covering 99% of PTV ($D_{99\%} > 90\%$), less than 5% of PTV getting 105% of the prescription dose ($V_{105\%} < 5\%$), and less than 110% of the prescription dose to 0.1cc volume of PTV ($D_{0.1cc} < 110\%$), as outlined by the MR-Linac consortium clinical treatment planning document.

Conventional Linac plans were generated using ≥ 7 coplanar non-opposing step-and-shoot IMRT 6 MV photon beams, with an additional non-coplanar beam if additional dose optimization was needed, as per standard of care. Maximum dose rate was 500 MU/min, and beam collimation used 80 MLC leaf pairs with a leaf width of 5 mm at isocenter. Plans were optimized to achieve at least 95% of PTV covered by 95% of the prescription dose ($V_{95\%} \geq 95\%$), and at most 1% of PTV getting 105% of the prescription dose ($V_{105\%} \leq 1\%$). All Monte Carlo dose calculations were as per institutional protocol to ensure that the total uncertainty at the dose reference point is less than

0.5%. Dose to OARs were constrained according to our institutional protocols (Supplemental Material, Table 1).

MR-Linac Monaco plans and conventional Linac Pinnacle plans for each patient were evaluated using cumulative dose-volume histogram (DVH) (Figure 2) parameters chosen a priori. For targets, dosimetric parameters of interest were extracted and compared from reference plans for the PTV, CTV, and GTV, including: (1) Volumes of tissue receiving at least 100%, 95%, 50% of the prescription dose ($V_{100\%}$, $V_{95\%}$, $V_{50\%}$); and (2) Minimum doses to 2%, 5%, 50%, 95%, 98% of the target volume ($D_{2\%}$, $D_{5\%}$, $D_{50\%}$, $D_{95\%}$, $D_{98\%}$). Dose homogeneity was assessed using homogeneity index (HI; Supplemental Material, Equation 1), with lower HI values (closer to 0) indicating more homogeneous dose distribution. Dose falloff outside of the target was assessed using gradient index (GI; Supplemental Material, Equation 2), with lower GI values characterizing a sharper dose falloff outside of the target. Dose conformity was assessed using conformity index (CI; Supplemental Material, Equation 3), with CI values closer to 1.0 signifying better conformity. OARs for each patients' clinical treatment plans were extracted and compared including: Maximum dose to 0.03cc volume of Lens, Globe, Optic chiasm, Optic nerve (Lens $D_{0.03cc}$, Globe $D_{0.03cc}$, Optic chiasm $D_{0.03cc}$, Optic nerve $D_{0.03cc}$), Maximum dose to 0.01cc volume of Brainstem (Brainstem $D_{0.01cc}$), and Mean dose to each cochlea (Cochlea D_{mean}). The maximum dose to a small but finite volume of an OAR was defined in order to partially manage the statistical noise inherent in a Monte Carlo TPS.

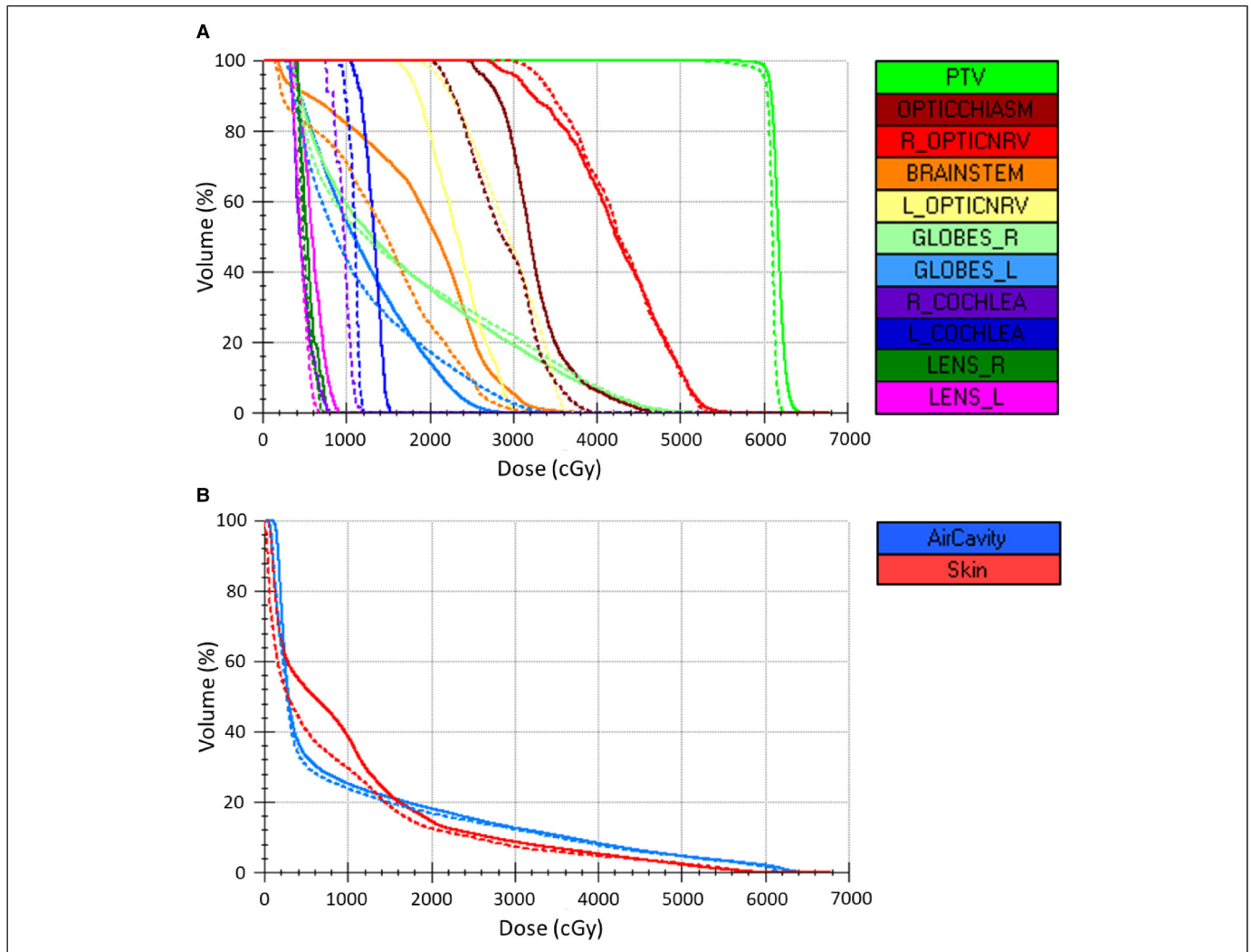


Figure 2. Dose-volume histograms of planning target volume and organs-at-risk (A), as well as tissues surrounding air cavities and at skin surface (B) for a representative study patient. Delivered MR-Linac treatment (solid lines) is compared with conventional Linac treatment (dashed lines).

For our study, skin volumes were generated as a 5 mm rim of tissue contracted from the patient body surface (Supplemental Material, Figure 1). Tissues around air cavities were generated as a 5 mm rim of tissue expanded from air cavity volumes (eg, nasopharynx, paranasal sinuses). Dosimetric parameters analyzed included: Mean dose and Maximum dose to 2cc volumes of tissues surrounding air cavities and skin contours (Air cavity Dmean, Air cavity D2cc, Skin Dmean, Skin D2cc), as well as the volume of skin receiving 20 Gy (Skin V20Gy).

For 10 randomly selected patients, *in vivo* skin dose measurements during one fraction of MR-Linac treatment and one fraction of conventional Linac treatment were obtained for the same patient using Optically Stimulated Luminescent Dosimeters (OSLDs; nanoDots, Landauer) placed in a defined location on the patient's skin near the PTV (Supplemental Material, Figure 2). Our institution has done extensive OSLD surface dose measurements previously to characterize and benchmark Monaco's Monte Carlo dose calculation engine and has

cross-validated OSLD measurements with other methods.^{9, 12, 25} Ideal OSLD positions were selected in the TPS at locations near the PTV, where the thermoplastic mask touches the skin. The TPS coordinates of the OSLD relative to the treatment isocenter was noted. The thermoplastic mask was setup on the treatment unit, and with the aid of a 3-dimensional laser positioning system, the OSLD locations were identified on the mask and the OSLD taped to the inside. OSLD dose point in the TPS was defined as the placement location on the treatment unit, at 0.6 mm depth from the patient surface. In the TPS, the patient surface was defined as the 0.6 g/cc boundary between tissue and air. A point dose was selected at a depth of 0.6 mm, with the mean dose within a radius of 0.1 mm about the point reported as the calculated dose. The 0.6 mm depth is the water equivalent depth of an OSLD taking into account its plastic casing, and the accuracy was rated to be $\pm 3\%$.¹² Dose delivered to skin, as measured by the OSLD, were correlated to both corresponding clinical treatment plans to determine which TPS best predicted the *in vivo* dose measurement.

Descriptive statistics were used to summarize the dosimetric parameters. Assumption of normality was assessed using the Smirnov–Kolmogorov test. Student's *t*-paired test or Wilcoxon signed-rank test, as appropriate based on normality assumption, were used to compare dosimetric parameters between MR-Linac plans and conventional Linac plans. Spearman's correlation was used to assess the relationship between in vivo OSLD measurements and TPS skin dose. All statistical tests were 2-sided, and threshold used for statistical significance was $P < .05$. Statistical analyses were performed using version 9.4 of the SAS system for Windows (2002-2012 SAS Institute, Inc.).

Results

Patient Population

Thirty-seven glioma patients treated with at least one fraction on both the MR-Linac and conventional Linac met study criteria and were analyzed. Baseline patient characteristics of patients included in the analyses are listed in Table 1.

Table 1. Patient Characteristics.

Characteristic	Total (N = 37)
Age	
<60 years	22 (59.5%)
60-69 years	7 (18.9%)
≥70 years	8 (21.6%)
Gender	
Male	25 (67.6%)
Female	12 (32.4%)
WHO grade	
II	9 (24.3%)
III	4 (10.8%)
IV	24 (64.9%)
Prescription	
40 Gy in 15 fractions	8 (21.6%)
54 Gy in 30 fractions	15 (40.5%)
60 Gy in 30 fractions	13 (35.1%)
59.4 Gy in 33 fractions	1 (2.7%)

Target Volumes and Organs-at-Risk

Comparisons of PTV dosimetric parameters between MR-Linac and conventional Linac plans are detailed in Table 2. There is no statistical difference in PTV V100%, V95%, V50%, D98%, and D95% ($P > .05$). Small but statistically significant differences were observed in mean PTV D50% ($P < .0001$), D5% ($P < .0001$), and D2% ($P < .0001$) for MR-Linac plans compared with conventional Linac. MR-Linac dose distributions had lower HI ($P = .0007$), better CI ($P = .0064$), and equivalent GI ($P > .05$) compared to conventional Linac.

Comparison of OAR dosimetric parameters between MR-Linac and conventional Linac plans is shown in Figure 2a, and summarized in Table 3. There was no statistical difference in the D0.03cc for the optic chiasm and optic nerves ($P > .05$), and no statistical difference in the mean dose to each cochlea ($P > .05$). Small but statistically significant differences were observed in clinically delivered D0.03cc for brainstem ($P = .0307$), D0.03cc for each globe ($P < .0010$), and D0.03cc for each lens ($P < .0001$) for the MR-Linac.

Tissues Around Air Cavities and at Skin Surface

The difference in dosimetric parameters for tissues surrounding air cavities and skin between MR-Linac and conventional Linac plans are shown in Figure 2b, and summarized in Table 4. For tissues surrounding air cavities, MR-Linac plans had statistically significant higher Dmean ($P < .0001$) and D2cc ($P = .0007$) compared to conventional Linac. For skin tissues, MR-Linac plans had statistically significant higher Dmean ($P < .0001$) and V20Gy ($P = .0001$) compared to conventional Linac, but no difference in D2cc ($P = .7975$).

Differences between predicted skin dose from the TPS and delivered skin dose measured from OSLD are quantified in Table 5. Mean skin dose as determined by the TPS was 7.8 Gy greater on MR-Linac plans (95% CI 3.7-11.8 Gy) compared with conventional Linac ($P = .0020$). Mean in vivo OSLD skin measurements were 4.6 Gy greater (14.5% higher) on MR-Linac treatments (95% CI 2.1-7.1 Gy) compared with conventional Linac ($P = .0027$). There was a

Table 2. Dosimetric Impact of Magnetic Field on Target Volume Parameters in Treated Glioma Patients.

PTV	MR-Linac (Mean ± ME)	Conventional Linac (Mean ± ME)	Paired difference (Mean ± ME)	<i>P</i> -value
V100% (cc)	265.94 ± 41.15	265.28 ± 41.43	0.66 ± 3.87	.9705
V95% (cc)	278.48 ± 42.19	269.44 ± 43.00	9.04 ± 14.54	.2920
V50% (cc)	280.07 ± 42.19	279.96 ± 42.17	0.11 ± 0.18	.5000
D98% (Gy)	52.19 ± 2.46	51.57 ± 2.43	0.62 ± 0.66	.5786
D95% (Gy)	53.11 ± 2.50	52.67 ± 2.47	0.44 ± 0.46	.1090
D50% (Gy)	54.67 ± 2.57	54.39 ± 2.57	0.27 ± 0.10	<.0001
D5% (Gy)	55.92 ± 2.63	55.17 ± 2.60	0.75 ± 0.12	<.0001
D2% (Gy)	56.28 ± 2.65	55.42 ± 2.61	0.86 ± 0.12	<.0001
Homogeneity index	1.05 ± 0.01	1.05 ± 0.02	0.01 ± 0.01	.0007
Gradient index	1.07 ± 0.04	1.22 ± 0.33	-0.14 ± 0.29	.8303
Conformity index	0.87 ± 0.02	0.83 ± 0.03	0.04 ± 0.03	.0064

ME = margin of error for 95% CI; Paired difference = MR-Linac – conventional Linac.

Table 3. Dosimetric Impact of Magnetic Field on Organs-at-Risk (OARs) in Treated Glioma Patients.

OARs	MR-Linac (Mean \pm ME)	Conventional Linac (Mean \pm ME)	Paired difference (Mean \pm ME)	P-value
Brainstem D0.1cc (Gy)	47.27 \pm 4.48	46.72 \pm 4.58	0.55 \pm 0.79	.0307
Optic Chiasm D0.03cc (Gy)	43.88 \pm 4.78	42.78 \pm 5.24	1.11 \pm 1.17	.5635
Optic Nerve Right D0.03cc (Gy)	35.47 \pm 5.64	35.36 \pm 6.09	0.11 \pm 1.38	.1804
Optic Nerve Left D0.03cc (Gy)	34.29 \pm 5.87	34.64 \pm 6.14	-0.35 \pm 1.26	.4858
Globe Right D0.03cc (Gy)	24.90 \pm 4.51	21.87 \pm 4.61	3.03 \pm 1.69	.0009
Globe Left D0.03cc (Gy)	22.26 \pm 3.54	18.56 \pm 3.48	3.70 \pm 1.98	.0005
Cochlea Right Dmean (Gy)	18.25 \pm 6.70	18.56 \pm 6.53	-0.30 \pm 1.78	.5597
Cochlea Left Dmean (Gy)	15.52 \pm 6.94	16.39 \pm 7.05	-0.87 \pm 1.80	.5046
Lens Right D0.03cc (Gy)	7.15 \pm 0.79	5.25 \pm 0.79	1.89 \pm 0.67	<.0001
Lens Left D0.03cc (Gy)	7.43 \pm 0.75	5.29 \pm 0.85	2.14 \pm 0.71	<.0001

ME = margin of error for 95% CI; Paired difference = MR-Linac – conventional Linac.

Table 4. Dosimetric Impact of Magnetic Field on Tissues Surrounding Air Cavities and at Skin Surface in Treated Glioma Patients.

Tissues surrounding air cavities and at skin surface	MR-Linac (Mean \pm ME)	Conventional Linac (Mean \pm ME)	Paired difference (Mean \pm ME)	P-value
Air Cavity Dmean (Gy)	12.05 \pm 2.27	10.53 \pm 2.08	1.52 \pm 0.60	<.0001
Air Cavity D2cc (Gy)	41.78 \pm 6.10	40.55 \pm 6.44	1.23 \pm 0.98	.0007
Skin Dmean (Gy)	8.64 \pm 1.99	7.54 \pm 2.00	1.10 \pm 0.54	<.0001
Skin D2cc (Gy)	45.55 \pm 2.80	45.45 \pm 3.67	0.11 \pm 0.85	.7975
Skin V20Gy (cm ³)	85.59 \pm 13.70	66.55 \pm 12.16	19.04 \pm 11.45	.0001

ME = margin of error for 95% CI; Paired difference = MR-Linac – conventional Linac.

Table 5. Comparison of Predicted Skin Dose From TPS Software and Delivered Skin Dose Measured From OSLD.

Skin dose	MR-Linac (Mean \pm ME)	Conventional Linac (Mean \pm ME)	Mean difference (Mean \pm ME)	P-value
TPS (Gy)	35.0 \pm 7.7	27.2 \pm 6.8	7.8 \pm 4.1	.0020
OSLD (Gy)	36.3 \pm 9.6	31.7 \pm 8.8	4.6 \pm 2.5	.0027
Mean difference	1.4 \pm 2.1	4.0 \pm 5.2		
P-value	Spearman $\rho = 0.9500$, $P < .0001$	Spearman $\rho = 0.8000$, $P < .0096$		

ME = margin of error for 95% CI.

1.4 Gy mean difference between MR-Linac Monaco modelled skin dose and in vivo OSLD measured skin dose. In contrast, there was a 4.0 Gy mean difference between conventional Linac Pinnacle modelled skin dose and in vivo OSLD measured skin dose. Furthermore, MR-Linac Monaco predicted in vivo OSLD measured skin dose more accurately (Spearman's correlation $\rho = 0.9500$, $P < .0001$). By comparison, there was a weaker association between conventional Linac Pinnacle modelled skin dose and in vivo OSLD measured skin dose (Spearman's correlation $\rho = 0.8000$, $P < .0096$).

Discussion

This is the first prospective dosimetric comparison of glioma patients clinically treated on both MR-Linac and conventional Linac and has several novel components. Our study's patient population uniquely represents a large cohort of glioma patients who received at least one fraction on both MR-Linac and

conventional Linac based on clinically approved radiotherapy plans. Furthermore, radiotherapy plans were prospectively generated prior to treatment and delivered on both MR-Linac and conventional Linac, in contrast to previous studies of simulated plans that were retrospectively generated for dosimetric comparison. Lastly and importantly, we performed in vivo skin dose measurements and determined that MR-Linac treatment plans had significantly greater skin doses, but were also better correlated with in vivo skin dose measurements.

We demonstrate that Monaco is able to accurately generate safe MR-Linac radiotherapy treatment plans for glioma patients that achieve planning objectives. We observed that with coplanar beam arrangements, MR-Linac treatments have lower homogeneity, but higher dose conformity and equivalent dose falloff outside of the target, when compared with conventional Linac. Conventional Linac with more coplanar beams, or additional non-coplanar beams could potentially achieve better dose falloff, but at the expense of greater monitor units and longer

treatment duration.²⁶ MR-Linac treatment plans had more heterogeneous dose distributions, which is consistent with the observed small but statistically significant increase in PTV D50%, D5%, and D2%. This is also consistent with previous reports showing higher heterogeneity and higher median V100% for MR-Linac plans compared with conventional Linac.²⁷ Similarly, a very small but statistically significant increase in Brainstem D0.1cc, each Globe D0.03cc, and each Lens D0.03cc was observed in MR-Linac plans. Over the course of a patient's entire radiotherapy regimen, the absolute summed dose difference was <1 Gy for PTV parameters, <1 Gy for brainstem, approximately 3 Gy for each globe, and approximately 2 Gy for each lens. Since MR-Linac treatment plans are adapted to position relative to intracranial soft tissues every fraction,²⁸ the exact location of these minimally higher dose regions varies geospatially every fraction, which may negate their effects when accumulated over the treatment course. All MR-Linac treatments achieved standard planning objectives and dose constraints, and it is unlikely that these small differences translate into clinically relevant outcomes.

We also quantitatively characterized the impact of the MR-Linac's magnetic field on delivered dose to skin and tissue surrounding air cavities. Compared to conventional Linac, we observed that MR-Linac treatments had 1.52 Gy higher Dmean ($P < .0001$), and 1.23 Gy higher D2cc ($P = .0007$) for tissues surrounding air cavities. Skin D2cc was not statistically different ($P > .05$), but skin Dmean was 1.10 Gy higher ($P < .0001$), and skin V20Gy was 19.04 cm³ higher ($P = .0001$) with MR-Linac treatment. This is consistent with recent preliminary studies investigating the effect of the MR-Linac's magnetic field on radiotherapy treatment.¹²⁻¹⁷ Tseng et al used Monaco to retrospectively generate MR-Linac plans with 9 coplanar non-opposing IMRT beams on 24 patients with intact single brain metastases, and found MR-Linac had 0.08 Gy higher Dmean and 0.6 Gy higher D2cc for skin, and 0.07 Gy higher Dmean and 0.3 Gy higher D2cc for tissues around air cavities.¹³ Schrenk et al used an open-source Monte Carlo-based TPS to retrospectively generate plans in the presence of a magnetic field with ≥ 7 coplanar non-opposing 3D-CRT and IMRT beams on 4 patients with non-small cell lung cancer, and found that the presence of the perpendicular magnetic field increased mean dose to tissues surrounding the lung air cavity by 0.5 Gy (18.5%).¹⁴ Nachbar et al used Monaco to prospectively generate a MR-Linac plan with 7 coplanar non-opposing IMRT beams on 1 breast cancer patient, and found MR-Linac had 0.3 Gy higher D2cc and 15.3% higher V35Gy for skin tissue.¹⁵ Xia et al used Monaco to retrospectively generate MR-Linac plans with 9 coplanar non-opposing equally spaced IMRT beams on 10 patients with hypopharyngeal cancer, and found MR-Linac had 1.30-1.81 Gy higher Dmean and 1.68-5.43 Gy higher Dmax for skin, and no difference in dose to tissues surrounding air cavities except for higher Dmax to larynx and trachea.¹⁶ Boldrini et al used MRIdian TPS to retrospectively generate MR-Linac plans with 7 coplanar non-opposing equally-spaced IMRT beams on 10 patients with locally advanced rectal cancer, and found MR-Linac had

higher skin dose and higher PTV V105% (14.8%) compared with conventional Linac VMAT with 2 full coplanar arcs (5.0%) and conventional Linac IMRT using 5 coplanar beams (7.3%).¹⁷ Taken together, these studies demonstrated that MR-Linac plans have small increases in dose to skin and tissues surrounding air cavities, and are consistent with our findings.

A potential limitation of our study is the variability in dose fractionations used. However, plan evaluation was performed with pairwise comparisons between MR-Linac and conventional Linac treatments for each patient and are independent of absolute values. Second, there may be potential uncertainty in OSLD measurements caused by placement, air gaps, and surface effects. To mitigate this, a single OSLD measurement was obtained from the same patient's MR-Linac and conventional Linac treatments using standardized technique,¹² although we acknowledge that reproducibility could be assessed by performing additional measurements. Third, we acknowledge that the MR-Linac and conventional Linac utilize different beam energies, different beam parameters, and different TPS to generate standard of care radiotherapy treatment plans that are clinically acceptable. There are differences in how each TPS models patient surface and calculates surface dosimetry. The true effect of the magnetic field on modelled skin dose remains unclear, and highlights the importance of OSLD measurements to properly compare skin surface doses between conventional Linac and MR-Linac treatments. Thus, our objective was to compare the skin dose from standard of care plans on each Linac individually and not an investigation to understand the underlying causes of differences in plan quality. Finally, each patient's clinically delivered treatment plan was analyzed on the latest version of clinical Monaco TPS, and we acknowledge that future iterations of clinical Monaco may have even better dose optimization, dose engines, and dose modelling.

Potential strategies to mitigate skin dose in MR-Linac treatment include increasing the number of beam angles,^{25, 29, 30} using opposing beam configurations,³¹ using VMAT,³² using partial arcs,³³ using smaller margins on target volumes,³⁴ and specifically using a skin structure objective during planning optimization to minimize skin dose. Kim et al investigated the effects of different beam arrangements on skin dosimetry for partial breast radiotherapy using MR-Linac, and demonstrated an 11% to 18% increase in skin D1cc and an 146% to 149% increase in skin V30 with the addition of the magnetic field. However, increasing the number of beam angles, and going from IMRT to VMAT reduced the skin dose in the presence of the magnetic field.³⁰ Bainbridge et al investigated the effect of a PTV margin reduction from 7 to 3 mm on skin dosimetry for lung cancer radiotherapy using MR-Linac. They demonstrated that MR-Linac plans with 7 mm margins had 0.4 Gy higher Dmean skin dose and 1.7 Gy higher D2cc skin dose compared to conventional Linac plans with 7 mm margins. However, MR-Linac plans with a reduced margin (3 mm) alleviated this issue, while also decreasing other OAR metrics, and allowed isotoxic dose escalation.³⁴

In glioblastoma, a phase I/II trial used a reduced 5 mm CTV margin with hypofractionated regimens and demonstrated survival outcomes similar to that of historical control.³⁵ Therefore, MRI-guided treatment of gliomas with a reduced CTV margin and an adaptive framework not only potentially mitigates skin dose effects on the MR-Linac, but may allow for opportunities to decrease toxicities and incorporate boost strategies based on functional imaging. Finally, since this study demonstrates that Monaco's Monte Carlo dose algorithm can accurately model the near-surface dose, using the TPS IMRT optimizer with skin as an avoidance structure can reliably decrease skin dose. Additional work to incorporate skin dose mitigation strategies into planning processes is being developed. Future work to prospectively assess dose-related clinical toxicity outcomes, such as wound dehiscence, permanent alopecia, and radiation dermatitis is important. Further studies investigating clinical scenarios where higher dose is required to skin and superficial targets are warranted as well.

Conclusion

This is the first prospective dosimetric comparison of glioma patients clinically treated with at least one fraction on both MR-Linac and conventional Linac, combined with in vivo correlation to delivered dose on each platform. We observed minimal dosimetric impact of the MR-Linac's magnetic field for target volumes and standard OARs. However, higher doses to tissues at skin surface and surrounding air cavities were observed for clinically delivered MR-Linac treatments. In vivo correlation of delivered skin dose suggests more accurate prediction in MR-Linac plans. Future MR-Linac planning processes are being designed to account for skin dosimetry and treatment delivery. Further work investigating MR-Linac dose-related clinical toxicities, and also clinical scenarios requiring higher dose to skin and superficial targets are important.

Declaration of Conflicting Interests

MR is a co-inventor/owns intellectual property specific to the image-guidance system on the Gamma Knife Icon outside the submitted work. HS has received travel accommodations/expenses and honoraria from Elekta AB outside the submitted work. SM has provided research support to Novartis AG and has received honoraria from Novartis AG and Ipsen and travel accommodations/expenses from Elekta outside the submitted work. BK has received previous grant funding from Elekta AB outside of the submitted work and has also received travel accommodations/expenses from Elekta AB outside of this work. AS is an advisor/consultant for AbbVie, Merck, Roche, Varian, Elekta AB, BrainLAB, and VieCure; is a board member of the International Stereotactic Radiosurgery Society; is a cochair of the AO Spine Knowledge Forum Tumor; has conducted educational seminars for Elekta AB, Accuray Inc, Varian, BrainLAB, and Medtronic Kyphon; has received research grants from Elekta AB and travel accommodations/expenses from Elekta AB, Varian, and BrainLAB; and is a member of the Elekta MR-Linac Research Consortium, Elekta Spine, Oligometastases, and Linac-based SRS Consortia. CLT has received travel accommodations/expenses and

honoraria from Elekta AB and belongs to the Elekta MR-Linac Research Consortium. The remaining authors declared no potential conflicts of interest with respect to the research, authorship, and/or publication of this article.

Funding

The authors received no financial support for the research, authorship, and/or publication of this article.

Ethics Approval

Ethical approval to report this study was obtained from the Research Ethics Board of Sunnybrook Health Sciences Centre, Toronto, Canada (Study Number: 3039).

Informed Consent

Written informed consent was obtained from all patients prior to enrollment for their de-identified information to be published in this article.

Clinical Trial

Study Name: Evaluation of Treatment, Imaging and Clinical Outcomes on the MR-Linac. Study Number: 3039.

ORCID iDs

Eshetu G. Atenafu  <https://orcid.org/0000-0002-4613-3680>
Chia-Lin Tseng  <https://orcid.org/0000-0002-3700-0886>

Supplemental Material

Supplemental material for this article is available online.

References

1. Stewart J, Sahgal A, Lee Y, et al. Quantitating interfraction target dynamics during concurrent chemoradiation for glioblastoma: a prospective serial imaging study. *Int J Radiat Oncol Biol Phys.* 2021;109(3):736-746. doi: 10.1016/j.ijrobp.2020.10.002. Epub 2020 Oct 14. PMID: 33068687.
2. Maralani PJ, Myrehaug S, Mehrabian H, et al. Intravoxel incoherent motion (IVIM) modeling of diffusion MRI during chemoradiation predicts therapeutic response in IDH wildtype glioblastoma. *Radiother Oncol.* 2021;156(1):258-265. doi: 10.1016/j.radonc.2020.12.037. Epub 2021 Jan 5. PMID: 33418005; PMCID: PMC8186561.
3. Raaymakers BW, Raaijmakers AJ, Kotte AN, Jette D, Lagendijk JJ. Integrating a MRI scanner with a 6 MV radiotherapy accelerator: Dose deposition in a transverse magnetic field. *Phys Med Biol.* 2004;49(17):4109-4118. doi: 10.1088/0031-9155/49/17/019. PMID: 15470926.
4. Chen X, Prior P, Chen GP, Schultz CJ, Li XA. Technical note: dose effects of 1.5 T transverse magnetic field on tissue interfaces in MRI-guided radiotherapy. *Med Phys.* 2016;43(8):4797. doi: 10.1118/1.4959534. PMID: 27487897.
5. Hackett SL, van Asselen B, Wolthaus JWH, et al. Spiraling contaminant electrons increase doses to surfaces outside the photon beam of an MRI-linac with a perpendicular magnetic field. *Phys Med Biol.* 2018;63(9):095001. doi: 10.1088/1361-6560/aaba8f. PMID: 29595150.

6. Huang CY, Yang B, Lam WW, et al. Effects on skin dose from unwanted air gaps under bolus in an MR-guided linear accelerator (MR-linac) system. *Phys Med Biol.* 2021;66(6):065021. doi: 10.1088/1361-6560/abe837. PMID: 33607641.
7. Ahmad SB, Sarfehnia A, Kim A, Wronski M, Sahgal A, Keller BM. Backscatter dose effects for high atomic number materials being irradiated in the presence of a magnetic field: a Monte Carlo study for the MRI linac. *Med Phys.* 2016;43(8):4665-4673. doi: 10.1118/1.4955175. PMID: 27487883.
8. Ahmad SB, Sarfehnia A, Paudel MR, et al. Evaluation of a commercial MRI Linac based Monte Carlo dose calculation algorithm with GEANT4. *Med Phys.* 2016;43(2):894-907. doi: 10.1118/1.4939808. PMID: 26843250.
9. Paudel MR, Kim A, Sarfehnia A, et al. Experimental evaluation of a GPU-based Monte Carlo dose calculation algorithm in the Monaco treatment planning system. *J Appl Clin Med Phys.* 2016;17(6):230-241. doi: 10.1120/jacmp.v17i6.6455. PMID: 27929496; PMCID: PMC5690498.
10. Raaijmakers AJ, Hårdemark B, Raaymakers BW, Raaijmakers CP, Lagendijk JJ. Dose optimization for the MRI-accelerator: IMRT in the presence of a magnetic field. *Phys Med Biol.* 2007;52(23):7045-7054. doi: 10.1088/0031-9155/52/23/018. Epub 2007 Nov 15. PMID: 18029992.
11. Raaijmakers AJ, Raaymakers BW, Lagendijk JJ. Integrating a MRI scanner with a 6 MV radiotherapy accelerator: dose increase at tissue-air interfaces in a lateral magnetic field due to returning electrons. *Phys Med Biol.* 2005;50(7):1363-1376. doi: 10.1088/0031-9155/50/7/002. Epub 2005 Mar 16. PMID: 15798329.
12. Kim A, Lim-Reinders S, Ahmad SB, Sahgal A, Keller BM. Surface and near-surface dose measurements at beam entry and exit in a 1.5 T MR-Linac using optically stimulated luminescence dosimeters. *Phys Med Biol.* 2020;65(4):045012. doi: 10.1088/1361-6560/ab64b6. PMID: 31860896.
13. Tseng CL, Eppinga W, Seravalli E, et al. Dosimetric feasibility of the hybrid magnetic resonance imaging (MRI)-Linac system (MRL) for brain metastases: The impact of the magnetic field. *Radiother Oncol.* 2017;125(2):273-279. doi: 10.1016/j.radonc.2017.09.036. Epub 2017 Oct 24. PMID: 29079310.
14. Schrenk O, Spindeldreier CK, Burigo LN, Hoerner-Rieber J, Pfaffenberger A. Effects of magnetic field orientation and strength on the treatment planning of nonsmall cell lung cancer. *Med Phys.* 2017;44(12):6621-6631. doi: 10.1002/mp.12631. Epub 2017 Nov 20. PMID: 29064573.
15. Nachbar M, Mönnich D, Boeke S, et al. Partial breast irradiation with the 1.5 T MR-Linac: First patient treatment and analysis of electron return and stream effects. *Radiother Oncol.* 2020;145(1):30-35. doi: 10.1016/j.radonc.2019.11.025. Epub 2019 Dec 23. PMID: 31874347.
16. Xia W, Zhang K, Li M, et al. Impact of magnetic field on dose distribution in MR-guided radiotherapy of head and neck cancer. *Front Oncol.* 2020;10:1739. doi: 10.3389/fonc.2020.01739. Erratum in: *Front Oncol.* 2020 Nov 13;10(1):604231. PMID: 33014859; PMCID: PMC7506127.
17. Boldrini L, Placidi E, Dinapoli N, et al. Hybrid Tri-Co-60 MRI radiotherapy for locally advanced rectal cancer: an in silico evaluation. *Tech Innov Patient Support Radiat Oncol.* 2018;6(1):5-10. doi: 10.1016/j.tipsro.2018.02.002. PMID: 32095572; PMCID: PMC7033778.
18. de Mol van Otterloo SR, Christodouleas JP, Blezer ELA, et al. The MOMENTUM study: an international registry for the evidence-based introduction of MR-guided adaptive therapy. *Front Oncol.* 2020;10(1):1328. doi: 10.3389/fonc.2020.01328. PMID: 33014774; PMCID: PMC7505056.
19. von Elm E, Altman DG, Egger M, Pocock SJ, Gøtzsche PC, Vandenbroucke JP; STROBE initiative. The strengthening the reporting of observational studies in epidemiology (STROBE) statement: guidelines for reporting observational studies. *Ann Intern Med.* 2007;147(8):573-577. doi: 10.7326/0003-4819-147-8-200710160-00010. PMID: 17938396.
20. Stupp R, Mason WP, van den Bent MJ, et al. European Organisation for Research and Treatment of Cancer Brain Tumor and Radiotherapy Groups; National Cancer Institute of Canada Clinical Trials Group. Radiotherapy plus concomitant and adjuvant temozolomide for glioblastoma. *N Engl J Med.* 2005;352(10):987-996. doi: 10.1056/NEJMoa043330. PMID: 15758009.
21. Perry JR, Laperriere N, O'Callaghan CJ, et al.; Trial Investigators. Short-course radiation plus temozolomide in elderly patients with glioblastoma. *N Engl J Med.* 2017;376(11):1027-1037. doi: 10.1056/NEJMoa1611977. PMID: 28296618.
22. Bol GH, Kotte AN, van der Heide UA, Lagendijk JJ. Simultaneous multi-modality ROI delineation in clinical practice. *Comput Methods Programs Biomed.* 2009;96(2):133-140. doi: 10.1016/j.cmpb.2009.04.008. Epub 2009 May 13. PMID: 19443076.
23. Tseng CL, Stewart J, Whitfield G, et al. Glioma consensus contouring recommendations from a MR-Linac international consortium research group and evaluation of a CT-MRI and MRI-only workflow. *J Neurooncol.* 2020;149(2):305-314. doi: 10.1007/s11060-020-03605-6. Epub 2020 Aug 29. PMID: 32860571; PMCID: PMC7541359.
24. Hissoiny S, Ozell B, Bouchard H, Després P. GPUMCD: A new GPU-oriented Monte Carlo dose calculation platform. *Med Phys.* 2011;38(2):754-764. doi: 10.1118/1.3539725. PMID: 21452713.
25. Lim-Reinders S, Keller BM, Sahgal A, Chugh B, Kim A. Measurement of surface dose in an MR-Linac with optically stimulated luminescence dosimeters for IMRT beam geometries. *Med Phys.* 2020;47(7):3133-3142. doi: 10.1002/mp.14185. Epub 2020 May 27. PMID: 32302010.
26. Panet-Raymond V, Ansbacher W, Zavgorodni S, et al. Coplanar versus noncoplanar intensity-modulated radiation therapy (IMRT) and volumetric-modulated arc therapy (VMAT) treatment planning for fronto-temporal high-grade glioma. *J Appl Clin Med Phys.* 2012;13(4):3826. doi: 10.1120/jacmp.v13i4.3826. PMID: 22766954.
27. Winkel D, Bol GH, Werensteijn-Honingh AM, et al. Target coverage and dose criteria based evaluation of the first clinical 1.5 T MR-linac SBRT treatments of lymph node oligometastases compared with conventional CBCT-linac treatment. *Radiother Oncol.* 2020;146(1):118-125. doi: 10.1016/j.radonc.2020.02.011. Epub 2020 Mar 6. PMID: 32146257.
28. Ruschin M, Sahgal A, Tseng CL, Sonier M, Keller B, Lee Y. Dosimetric impact of using a virtual couch shift for online

- correction of setup errors for brain patients on an integrated high-field magnetic resonance imaging linear accelerator. *Int J Radiat Oncol Biol Phys.* 2017;98(3):699-708. doi: 10.1016/j.ijrobp.2017.03.004. Epub 2017 Mar 10. PMID: 28581412.
29. Raaijmakers AJ, Raaymakers BW, van der Meer S, Lagendijk JJ. Integrating a MRI scanner with a 6 MV radiotherapy accelerator: Impact of the surface orientation on the entrance and exit dose due to the transverse magnetic field. *Phys Med Biol.* 2007;52(4):929-939. doi: 10.1088/0031-9155/52/4/005. Epub 2007 Jan 22. PMID: 17264362.
30. Kim A, Lim-Reinders S, McCann C, et al. Magnetic field dose effects on different radiation beam geometries for hypofractionated partial breast irradiation. *J Appl Clin Med Phys.* 2017;18(6):62-70. doi: 10.1002/acm2.12182. Epub 2017 Sep 13. PMID: 28901729; PMCID: PMC5689934.
31. Bol GH, Lagendijk JJ, Raaymakers BW. Compensating for the impact of non-stationary spherical air cavities on IMRT dose delivery in transverse magnetic fields. *Phys Med Biol.* 2015;60(2):755-768. doi: 10.1088/0031-9155/60/2/755. Epub 2015 Jan 5. PMID: 25559321.
32. Audet C, Poffenbarger BA, Chang P, et al. Evaluation of volumetric modulated arc therapy for cranial radiosurgery using multiple noncoplanar arcs. *Med Phys.* 2011;38(11):5863-5872. doi: 10.1118/1.3641874. PMID: 22047350.
33. Davidson MT, Masucci GL, Follwell M, et al. Single arc volumetric modulated arc therapy for complex brain gliomas: is there an advantage as compared to intensity modulated radiotherapy or by adding a partial arc? *Technol Cancer Res Treat.* 2012;11(3):211-220. doi: 10.7785/tcrt.2012.500289. Epub 2012 Mar 1. PMID: 22376134.
34. Bainbridge HE, Menten MJ, Fast MF, Nill S, Oelfke U, McDonald F. Treating locally advanced lung cancer with a 1.5 T MR-Linac - Effects of the magnetic field and irradiation geometry on conventionally fractionated and isotoxic dose-escalated radiotherapy. *Radiother Oncol.* 2017;125(2):280-285. doi: 10.1016/j.radonc.2017.09.009. Epub 2017 Oct 4. PMID: 28987747; PMCID: PMC5710994.
35. Azoulay M, Chang SD, Gibbs IC, et al. A phase I/II trial of 5-fraction stereotactic radiosurgery with 5-mm margins with concurrent temozolomide in newly diagnosed glioblastoma: primary outcomes. *Neuro Oncol.* 2020;22(8):1182-1189. doi: 10.1093/neuonc/noaa019. PMID: 32002547; PMCID: PMC7594571.